A resorbable antibiotic eluting bone void filler for periprosthetic joint infection prevention

Zachary Jones,[1] Amanda E. Brooks,[1,2]* Zachary Ferrell,[1] David W. Grainger,[1,3]
Kristofer D. Sinclair[2]

[1]Department of Bioengineering, University of Utah, Salt Lake City, Utah 84112
[2]Elute Inc, Salt Lake City, Utah 84108
[3]Department of Pharmaceutics and Pharmaceutical Chemistry, University of Utah, Salt Lake City, Utah 84112

Abstract: Periprosthetic joint infection (PJI) following total knee arthroplasty is a globally increasing procedural complication. These infections are difficult to treat and typically require revision surgery. Antibiotic-loaded bone cement is frequently utilized to deliver antibiotics to the site of infection; however, bone cement is a nondegrading foreign body and known to leach its antibiotic load, after an initial burst release, at subtherapeutic concentrations for months. This work characterized a resorbable, antibiotic-eluting bone void filler designed to restore bone volume and prevent PJI. Three device formulations were fabricated, consisting of different combinations of synthetic inorganic bone graft material, degradable polymer matrices, salt porogens, and antibiotic tobramycin. These formulations were examined to determine the antibiotic's elution kinetics and bactericidal potential, the device's degradation *in vitro*, as well as osteoconductivity and device resorption *in vivo* using a pilot rabbit bone implant model. Kirby-Bauer antibiotic susceptibility tests assessed bactericidal activity. Liquid chroma-tography with tandem mass spectrometry measured antibiotic elution kinetics, and scanning electron microscopy was used to qualitatively assess degradation. Results indicated sustained antibiotic release from all three formulations above the *Staphylococcus aureus* minimum inhibitory concentration for a period of 5 to 8 weeks. Extensive degradation was observed with the Group 3 formulation after 90 days in phosphate-buffered saline, with a lesser degree of degradation observed in the other two formulations. Results from the pilot rabbit study showed the Group 3 device to be biocompatible, with minimal inflammatory response and no fibrous encapsulation in bone. The device was also highly osteoconductive—exhibiting an accelerated mineral apposition rate. © 2015 Wiley Periodicals, Inc. J Biomed Mater Res Part B: Appl Biomater 00B: 000–000, 2015.

Key Words: preclinical rabbit animal model, total joint revision, controlled drug release, tobramycin, osteomyelitis

How to cite this article: Jones Z, Brooks AE, Ferrell Z, Grainger DW, Sinclair KD. 2015. A resorbable antibiotic eluting bone void filler for periprosthetic joint infection prevention. J Biomed Mater Res Part B 2015:00B:000–000.

INTRODUCTION

Periprosthetic joint infection (PJI) following total knee arthroplasty (TKA) is a growing concern in the United States; affecting approximately 2% of patients.[1] It is estimated that PJI will affect 60,000 to 70,000 patients per year by the year 2020 at an annual cost exceeding 1.6 billion dollars.[2] Despite antibiotic treatment of 6 weeks or more, many of these infections are not eradicated, leaving invasive surgical intervention and replacement arthroplasty as the most common interventions.[3] In these cases a two-stage resection arthroplasty with hardware exchange is commonly performed. The prosthetic hardware is removed and the affected area is extensively debrided; following debridement, numerous voids are often left in the bone. These are commonly filled with nondegradable antibiotic-loaded bone cement (ALBC), a nondegradable poly(methyl methacrylate) polymer and foreign body that cannot release its antibiotic load very effectively.[4,5] Even after this costly and lengthy process, infection recurs in approximately 15% of these patients.[1]

Clinical use of systemic antibiotics and ALBC has several shortcomings. First, PJI is difficult to treat due to limited antibiotic perfusion to the site of infection.[6] This is further complicated by the formation of sequestra,[7] which form when pieces of necrotic bone are separated from healthy, viable bone. Resident bacteria can also form biofilm, protected by dense polysaccharide matrices that shelter them from host immune responses and antimicrobial agents.[8] Consequently, high concentrations of antibiotics, which produce myriad side effects attributable to toxicity, are required to treat PJI.[9] Finally, ALBC lacks osteoconductivity, serves as a foreign body for bacterial adhesion,[10] and can elute

*Present address: Department of Pharmaceutical Sciences, North Dakota State University, Fargo, ND 58102, USA
Correspondence to: K.D. Sinclair; e-mail: kristofer.sinclairkristof@gmail.com

TABLE I. Material Composition of the Four ABVF Groups for Determination of *In Vitro* Efficacy

	Study Groups—Material % Composition					
Group	ProOsteon® 500R (%)	PCL (%)	PEG (%)	CaCl$_2$ (%)	PLGA (%)	Tobramycin (%)
1	63.1	24.3	2.7	0	0	10.0
2	60.6	23.4	2.6	3.8	0	9.5
3	60.7	7.4	3.7	3.8	14.8	9.5
4	67.1	8.2	4.1	4.3	16.4	0

antibiotic for long durations at subtherapeutic levels—often resulting in the development of antibiotic resistant pathogens.[4,5]

The multiple shortcomings of the current approaches have led to exploration of other treatment options for PJI. Biodegradable polymers such as polycaprolactone (PCL), poly (lactide) (PLA), and poly(glycolide) (PGA), polyanhydrides, and polyurethaness have been studied as delivery vehicles for sustained, local release of antibiotics—directly to bone infection sites.[11–14] PCL has been used for sustained release of tobramycin in rabbit models,[15] and copolymers of PLA and PGA (PLGA) have been used in devices for sustained local delivery of gentamicin.[16] Resorbable devices, comprised of combinations of polymers, osteoconductive materials, and antibiotic, represent a promising approach to treating PJI.

The primary goal of this study was to design, characterize, and assess the efficacy of a resorbable, antibiotic-eluting bone void filler (ABVF) composed of synthetic calcium phosphate coralline inorganic granular bone graft (ProOsteon® 500R), biodegradable polymers (PCL, PEG, and PLGA), porogens (CaCl$_2$), and broad-spectrum antibiotic (tobramycin) for prevention of PJI (Table I). Specifically, the work described characterized the devices *in vitro*: bactericidal activity, antibiotic elution kinetics, and degradation; as well as a pilot *in vivo* assessment of the device's osteoconductivity. It was hypothesized that these devices would elute the antibiotic, tobramycin, at or above the minimum inhibitory concentration of >2 μg/mL for a period of 6 to 8 weeks[17] and would demonstrate bactericidal activity over the same, 6- to 8-week period of time *in vitro*. The second hypothesis was that these devices would exhibit significant signs of degradation in isotonic phosphate-buffered saline (PBS) within 90 days. Finally, we hypothesized that the resorbable, ABVF would demonstrate measurable osteoconductivity *in vivo* using a pilot rabbit radial window defect model. Currently, no implantable bone device is available for treating PJI that is both osteoconductive and capable of extended antibiotic delivery at therapeutic levels for 6 to 8 weeks.

MATERIALS

Polycaprolactone (PCL, 10,000 Da M_n, Sigma-Aldrich), polyethylene glycol (PEG, 20,000 Da, Sigma-Aldrich), ProOsteon® 500R calcium phosphate-hydroxyapatite coralline granules (150–425 μm diameter) (Biomet, Inc. Warsaw, IN), PLGA (50:50, 0.55–0.75 dL/g I.V., 31,300–57,600 Da, Lactel-Durect Corporation), calcium chloride solid granules (CaCl$_2$, sieved

to <250 μm; Sigma-Aldrich), and solid tobramycin (MP Biomedical) were all used as supplied.

METHODS
Polymer physical properties and device fabrication
Polymer stability. The physical properties of the polymers were analyzed using differential scanning calorimetry (DSC) to ensure the thermal stability of the polymers before device fabrication. Analysis was performed with a TA Instruments DSC Q200 (Newcastle, DE), using flat slices of polymer (~5 μg). The samples were placed individually into standard aluminum DSC pans, capped, crimped to seal, and placed into the Mettler ME 30 microbalance (Columbus, OH) to ascertain weight. Subsequently, samples were placed into a nitrogen-purged (flow rate of 40 mL/min) DSC individually. Temperature was ramped from −70°C (instrument cooling limit) to 200°C at a rate of 10°C/min for PCL and poly(ethylene glycol) (PEG) and −70°C to 325°C at a rate of 10°C/min for PLGA to measure the changes in heat capacity. Upon completion of the cycle, samples were removed, quenched with liquid nitrogen, and run through a second heating cycle. Quenching was performed to remove thermal history, allow visualization of the exothermic peak associated with crystallization, and to obtain crystallization temperatures.

Device fabrication. Four different formulations (three test formulations and one control) of resorbable, ABVF devices were fabricated as previously described[18] for evaluation of antibiotic release kinetics and bactericidal activity (Table I). Group 1 consisted of 135 mg of PCL, 15.0 mg of PEG, 350 mg of ProOsteon® 500R coralline granules, and 55 mg of powdered tobramycin. After materials were weighed, the PCL and PEG were melted and mixed at 75°C to uniformity. Once homogenized, ProOsteon® 500R (morselized and sieved to 150–425 μm)[18] was added to the molten mixture, mixed for uniformity, and then solid powdered tobramycin was incorporated into the molten matrix. The uniform polymer-ceramic composite was subsequently pressed into silicone molds (2 mm × 2 mm × 6 mm; Grace Bio-labs) and cooled to form solid blocks (that is, ABVF croutons) of uniform dimensions and densities.

Group 2 devices followed the same procedures as group I; however, to increase the porosity of the combination device, 22.2 mg of CaCl$_2$ (sieved to <250 μm; Sigma-Aldrich) was added to serve as a porogen. Calcium chloride

was added to the blend after the ProOsteon® 500R solid was mixed in, but before addition of tobramycin.

Group 3 devices consisted of 42.8 mg of PCL, 21.4 mg of PEG, 85.5 mg of PLGA, 350 mg of ProOsteon® 500R, 22.2 mg of $CaCl_2$, and 55.0 mg tobramycin. PLGA was added to increase the rate of device resorption. PLGA was dissolved into 400 μL of acetone and mixed in an Eppendorf Thermomixer (Hamburg, Germany) at 1400 rpm and 37°C. The preparation was performed in the same manner as group 2 devices with the PLGA/acetone solution added after tobramycin and before packing the molten matrix into the silicone mold.

The group 4 formulation was prepared in the same manner as group 3; however, no tobramycin was included in these devices for use as experimental controls. Each device (groups 1–4) was then characterized by measuring the mass and dimensions (length, width, and height) of each device. Each batch yielded approximately 10 devices for each of the four intended implant formulations.

Antibiotic elution kinetics. Devices ($n = 3$/group) from groups 1 to 4 were placed into 5 mL of sterile 1× (isotonic) PBS and incubated at 37°C for 10 weeks under aseptic conditions. During this 10-week study, aliquots of 1 mL were removed at 4, 8, and 24 h on the first day and then weekly thereafter, for the remainder of the 10-week study. For each 1 mL aliquot removed, the sampling volume was replenished with 1 mL of fresh PBS. Every 24 h, the PBS was removed, checked for changes in pH, and replaced with 5 mL of fresh PBS to preserve sink conditions. All aliquots were removed and stored at −80°C before analysis. Liquid chromatography with tandem mass spectrometry (LC-MS/MS—Waters Xevo G2S Q-ToF) was used to analyze the samples to determine the tobramycin concentration according to methods described by Keevil et al.[19]

Scanning electron microscopy. The devices' surface topography was ascertained qualitatively over the time course of buffer immersion using scanning electron microscopy (SEM). A previous *in vivo* study evaluating the group 1 device[20] reported that this device did not degrade *in situ*. Furthermore, the glassy surface of the device provoked a foreign body response resulting in the fibrous encapsulation of the device. Therefore, SEM was employed to evaluate the effects of PBS hydrolysis on the polymeric surface over time for each design. Devices ($n = 3$/group) from each group (groups 1–4) were incubated in 5 mL of PBS at 37°C for durations of 0, 30, 60, and 90 days to model *in vivo* degradation. Following removal from the PBS at the designated time point, samples were allowed to air dry for 1 week and were then imaged to assess surface topography.

In vitro microbiology
The minimum inhibitory concentration (MIC) and minimum bactericidal concentration (MBC) were determined for tobramycin with *Staphylococcus aureus* strain American Type Culture Collection (ATCC) 49230, human osteomyelitis clinical isolate,[21] before experimentation for the purpose of

understanding the concentrations necessary to inhibit bacterial growth. Tobramycin dilutions were prepared in cationic adjusted Mueller Hinton Broth (CAMHB) and added to a bacterial suspension containing 5×10^5 colony forming units (CFU)/ml (as determined with a nephelometer according to McFarland standards) in CAMHB to achieve a final volume of 2 mL and final concentrations of 0.5, 1.0, 2.0, 3.0, 4.0, 6.0, 8.0, 10.0, 12.0, 14.0, and 16.0 μg/mL of tobramycin.[22]

Kirby-Bauer antibiotic susceptibility testing. To determine bactericidal efficacy, a Kirby-Bauer zone of inhibition (ZOI) study was performed.[23] Five samples from each formulation (1 sample per each 2.0 mL volume of sterile 1× PBS) were incubated at 37°C. After 24 h, the solution was replaced with 2 mL of fresh PBS. This exchange process was repeated at 48 h and then once per week for a period of 10 weeks. Aliquots of 500 μL were removed at each time point and placed in a laminar flow hood to dry. After 24 h, the solutions were transferred to a 96-well plate containing #1 Whatman filter article punched to disks with a 6-mm diameter. The plate was left in the laminar flow hood to dry and then each filter article disk was placed on an agar plate on which a *S. aureus* ATCC 49230 suspension (0.5 McFarland) had been spread using a sterile cotton swab to create a confluent bacterial lawn. Bacterial suspensions were prepared in sterile 1× PBS and measurements were taken using a BD Medical (Sandy, UT) nephelometer based on optical density. After 24 h the ZOI around the antibiotic-laden filter article disks were measured using digital calipers.

Modified Kirby-Bauer antibiotic susceptibility study. A modified Kirby-Bauer ZOI study was developed to compare antibiotic release from resorbable ABVF devices (groups 1–4). Devices were placed into 2 mL PBS in an incubator at 37°C.Devices were removed at 0, 24, and 48 h, then weekly thereafter for the duration of the 12-week study. Each device was embedded in the center of the plate in agar within petri dishes. Embedding was accomplished by creating an incision within the agar using a sterile scalpel. Devices were then placed within the incision using sterile forceps, to a depth of ~2 mm. A 0.5 McFarland suspension of *S. aureus* was prepared and spread across the agar to create a continuous bacterial lawn. Samples were incubated for 24 h, after which the ZOI was measured. Each experiment was performed in triplicate.

Pilot *in vivo* osteoconductivity assessment
Study groups. The experimental protocol was approved by the Institutional Animal Care and Use Committee (IACUC) at the University of Utah. Based upon a previous, statistically powered *in vivo* study that demonstrated fibrous encapsulation of the group 1 device,[20] two rabbits were implanted with one sterile (STERRAD® sterilization; ETHICON, USA) group 3 device to test *Hypothesis 3*. The device was placed into a radial window defect created on the right forelimb, as described below. To obtain "Time 0" data, one group 3

TABLE II. Summary of dynamic histomorphometry measurements (value ± SE) for rabbits #102 and 103

	%dLs	%sLs	%MS	MAR (μm/day)	NBA (μm^2)
Periosteal measures					
102	5.35 ± 1.48	19.86 ± 6.14	15.28 ± 2.64	1.90 ± 0.45	21,845.29 ± 7720.62
103	40.61 ± 10.87	19.50 ± 5.20	50.36 ± 11.07	2.79 ± 0.12	177,459.43 ± 57,854.08
Endosteal measures					
102	12.46 ± 2.94	9.05 ± 4.53	16.98 ± 3.59	2.54 ± 0.15	23,745.75 ± 1907.86
103	26.89 ± 5.06	10.67 ± 4.21	32.23 ± 6.78	3.36 ± 0.23	41,736.85 ± 11,034.22

Both rabbits demonstrated a high rate of bone metabolic activity as shown in the table listed above.

device was implanted into the left radius of each rabbit at the time of necropsy.

Surgical procedure. Two (#102 and #103) skeletally mature male rabbits (4–5 months old, species New Zealand NZW rabbits, 4.5 kg ± 0.07 kg) were used in this study. All procedures were performed using aseptic surgical technique. A board-certified veterinarian administered analgesics and anesthetics and the rabbits were maintained under isofluorane (0.5–5%). The right forelimb was shaved at the surgical site, scrubbed for 10 min using standard betadine/alcohol scrub, and then prepped with Chloraprep (2% chlorhexidine gluconate/70% isopropanol). The cortical bone window defect (~6 mm × 2 mm × 2 mm) was created with a high-speed surgical drill with sterile saline cooling into the proximal medial diaphysis of the right radius. Bone marrow was removed by sterile saline lavage, the defect was filled with one sterilized group 3 device, and the fascia and skin were closed in layers over the cortical defect using 3.0 sutures. Once closed, the wound was cleaned with sterile saline and painted with betadine solution. The wound site was dressed with a non-stick Telfa pad and vet wrap.

In vivo end points. Following surgery and before the study's 12-week end point, calcein green (Sigma-Aldrich) was administered intravenously both 16 and 5 days before necropsy to fluorescently label calcifying new bone. Following euthanasia, hard and soft tissue samples were collected to characterize the surgical site via microbiologic and histologic techniques.

Explant micro-CT imaging. All samples were scanned on a volumetric micro-CT scanner (General Electric EVS-RS9). The image data were acquired at 50 μm isotropic voxel resolution, two frames, 70 kV, 114 μA, $t = 300$ ms. The micro-CT generated image slices were combined into an image volume using the Teem (http://teem.sourceforge.net/) software package. All datasets were cropped and reoriented to capture the same region with similar orientation. Rotating, volume-rendered movies of each 3D dataset were generated using SCIRun (Scientific Computing and Imaging Institute, University of Utah, UT).

Histomorphometric measurements. The radius was fixed in 10% buffered formalin, dehydrated using ascending concentrations of ethanol, and embedded in poly(methyl methacrylate) (PMMA).[24] Embedded samples were cut into

~2 mm sections, the samples were then ground and polished for SEM and backscatter SEM (BSE). BSE images were analyzed for signs of bone resorption, bone remodeling, porosity, woven bone formation, and bone ingrowth into the porous coated region.[25]

Following BSE, the PMMA sections of the bone were ground to allow light transparency (that is, 50–70 μm thickness). Fluorescence microscopy and BIOQUANT image analysis (BIOQUANT Corporation, Nashville) software were used to quantify mineral apposition rate (MAR) at various depths of the bone along the implant margins.[24] Histomorphometric analysis evaluated each sample for percent double-labeled surface (%dLs), percent single-labeled surface (%sLs), percent mineralizing surface (%MS), MAR (microns/day), and new bone area (NBA) (Table II).

Finally, histological sections were evaluated with Sanderson's Rapid bone stain. This provided qualitative data for different cells present at the implant/bone interface, i.e. the presence of osteoclasts, osteoblasts, immune cells, fibrous tissue formation, infection, and overall tissue morphology.[26] Implant host response was evaluated based upon the presence and quality of bone, fibrous tissue, and inflammatory cells throughout the bone-implant interface.
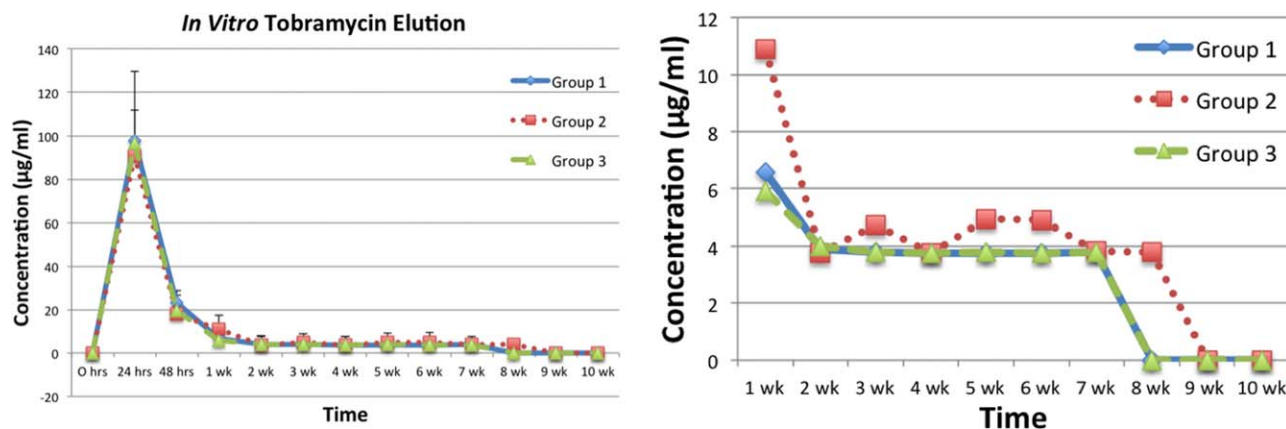
Statistical analysis. The mean and variance (standard error of the mean (SE)) for experimental populations were determined in order to demonstrate reproducibility in the results. Unpaired *t*-tests were used to determine statistical significance between experimental and control groups for elution kinetics, Kirby-Bauer, and modified Kirby-Bauer studies. Significance was deemed for *p* values <0.05. The *in vivo* animal study data were evaluated using survival analysis.

RESULTS
Polymer and device physical properties analysis
Device dimensions. Batches containing approximately 10 croutons each were fabricated for each group of antibiotic eluting bone void filler. Each device possessed the approximate: dimensions of 2 mm wide, 2 mm tall, and 6 mm long ±10%, drug load of 5.5 mg/device, and mass of 35 mg ± 5%.[18]

Differential scanning calorimetry. DSC data (not shown) demonstrated phase transitions for the materials used in this work to be similar to those reported in literature—
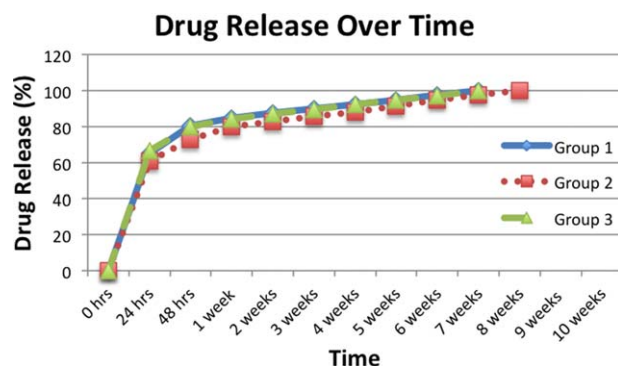
FIGURE 1. A) Tobramycin concentration is plotted versus time for the three device formulations. The data show a large initial release followed by a precipitous drop in drug release after 24 h. Drug release remained fairly consistent from week 1 to 7 in groups 1 & 3. B) An expanded view of weeks 1 to 10 from (A) is shown. [Color figure can be viewed in the online issue, which is available at wileyonlinelibrary.com.]

slight variances attributable to differences in molecular weight.[27–29] Peak melting temperature ranges for PCL and PEG were observed to be 65.8–69.0°C and 62.0–63.6°C, respectively. Known glass transition temperatures for these polymers (that is, PCL $T_g \sim -60$°C, and PEG ($T_g \sim -34$°C) were not detected due to the cooling limitations of the DSC equipment. Nonetheless, no indications of degradation/oxidation of either PCL or PEG during the experiment (maximum $T = 200$°C) were noted. PLGA demonstrated a glass transition temperature range of 42.4 to 44.1°C and a peak melting temperature range of 158 to 173°C. No evidence of PLGA degradation/oxidation was observed during the DSC run up to 325°C.

Compression testing. Compression testing was preformed to ensure that the sterilization process did not deleteriously effect device mechanical properties. Comparisons of sterilized and nonsterilized devices revealed that sterilization had no effect on compressive strength (data not shown).

Antibiotic elution kinetics. All three groups (groups 1–3) were observed to elute the antibiotic, tobramycin, above the

FIGURE 2. Cumulative tobramycin elution over the course of the 10-week *in vitro* study. A burst release was noticed over the first 48 hours, followed by a more gradual sustained release for 7 (groups 1 & 3) to 8 (group 2) weeks. [Color figure can be viewed in the online issue, which is available at wileyonlinelibrary.com.]
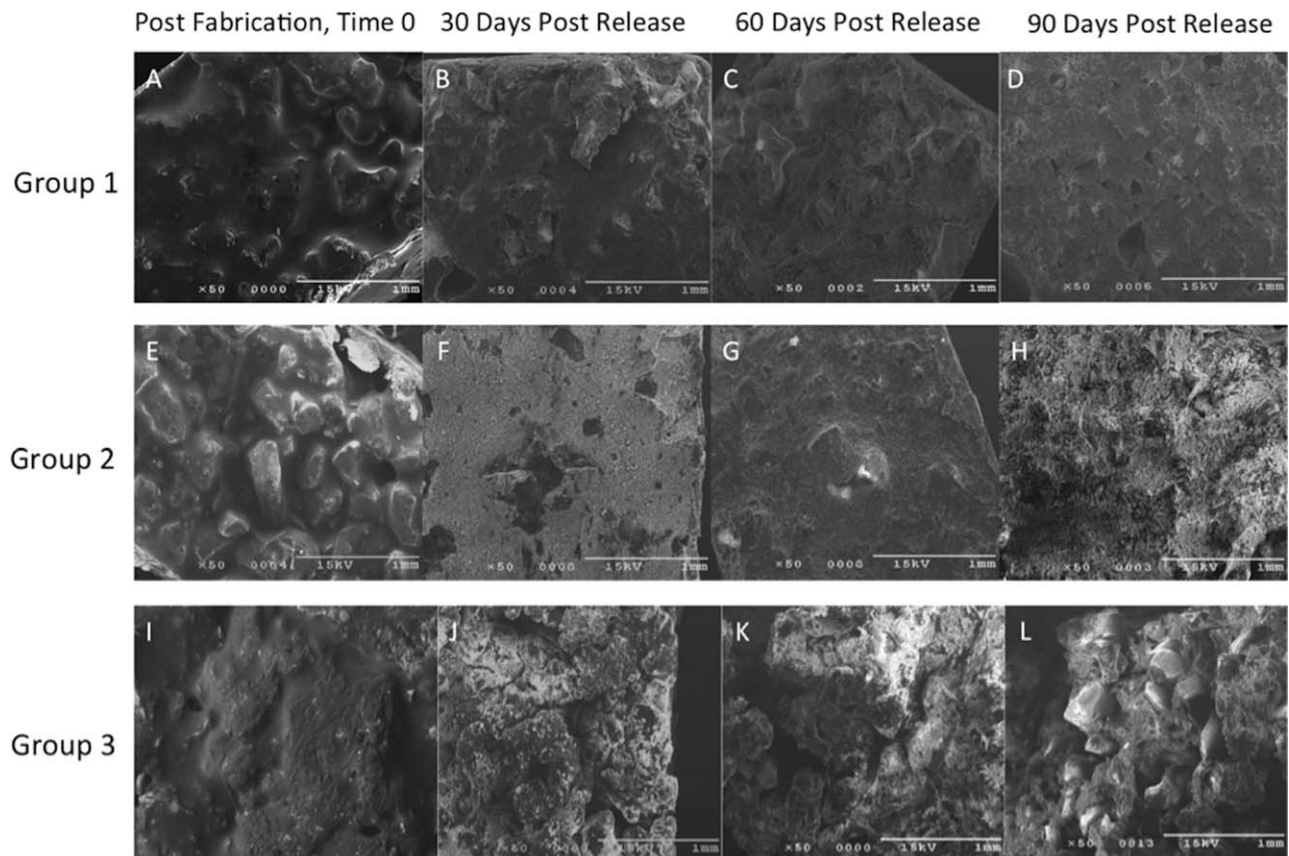
measured MBC for up to 7 weeks *in vitro* [Figure 1(A)]. At 24 h, tobramycin reached peak concentrations of 97.8 ± 6.8 μg/mL, 90.5 ± 19.6 μg/mL, and 96.4 ± 7.7 μg/mL for groups 1 to 3, respectively. At 7 weeks, tobramycin concentrations for all three groups were observed to be 3.8 ± 1.9 μg/mL [Figure 1(B)]. Group 2 devices showed measureable (3.8 μg/mL) tobramycin elution out to 8 weeks. However, no measureable tobramycin release was recorded for any group beyond 9 weeks (Figure 2).

Evaluation of pH revealed no change over the course of the 10-week study. The initial pH of 7.2 was observed with each daily solution exchange throughout the experiment.

Scanning electron microscopy. SEM surface analysis of ABVF devices revealed a glassy, nonporous polymer surface postfabrication in Time "0" samples—regardless of formulation Group [Figure 3(A,E,I)]. After 90 days in PBS, very little surface or bulk device degradation was observed in group 1 devices [Figure 3(D)]. Group 2 showed slightly more degradation than group 1 [Figure 3(H)]. Group 2 degradation was characterized by formation of pits as a result of $CaCl_2$ solubilization and leaching—numerous pits and polymer "flaking" around these pits was observed throughout the ABVF surfaces. Group 3 exhibited the greatest degree of degradation after 90 days in PBS [Figure 3(L)]. The surface of group 3 was highly eroded, containing numerous cracks and fissures, and revealed exposed ProOsteon inorganic coralline BVF granules.
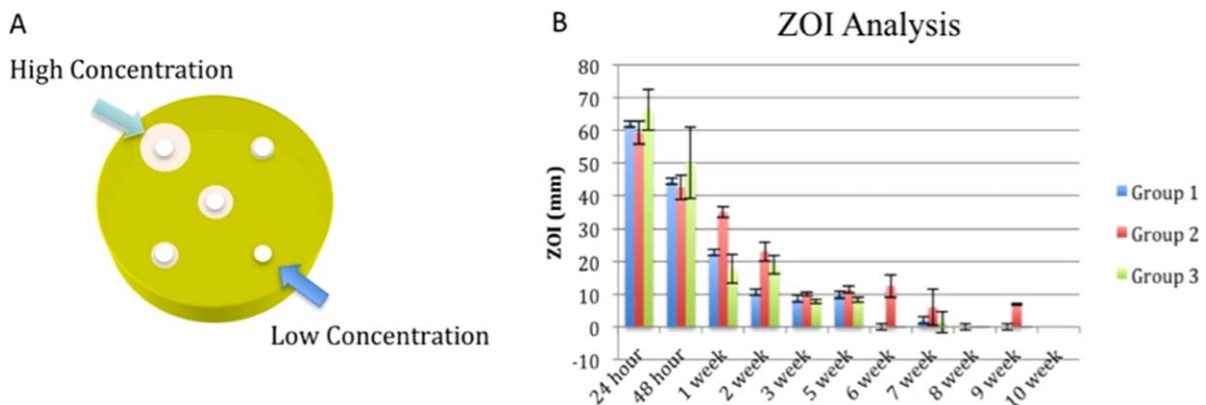
In vitro analyses

Tobramycin sensitivity. The results of the bacterial sensitivity testing for *S. aureus* strain ATCC 49230 revealed a minimum inhibitory concentration (MIC) of >2 μg/mL and a minimum bactericidal concentration (MBC) of 3 μg/mL. These experimentally determined values were lower than those reported (MIC = 4–8 μg/mL, MBC = 16 μg/mL),[30] but consistently reproduced.

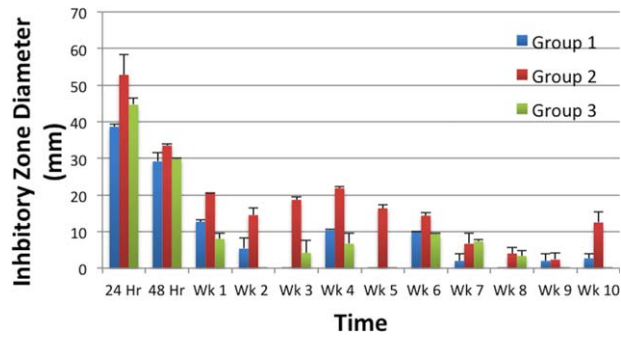Post Fabrication, Time 0   30 Days Post Release   60 Days Post Release   90 Days Post Release

FIGURE 3. SEM images comparing the aqueous *in vitro* degradation of ABVF devices exposed to PBS for up to 90 days, based upon fabrication group (see Table I) and the length of incubation in aqueous milieu. Degradation was more pronounced in group 3 than either of the other two groups.

Kirby-Bauer antibiotic susceptibility. Kirby-Bauer testing resulted in the production of measurable ZOIs for up to 8 weeks for Groups 1 and 3 (Figure 4). Group 2 continued to produce measurable ZOIs to 9 weeks [Figure 4(B)]. Average ZOI diameters at the 24-h time point were: 49.6 ± 2.6 mm, 58.7 ± 1.19 mm, and 53.0 ± 2.2 mm for groups 1 to 3, respectively; with group 2 demonstrating statistically greater ($p < 0.05$) inhibition than groups 1 and

3. Average ZOI diameters decreased for all three groups at 48 h and continued to diminish in diameter for the duration of the study. At week 7, diameters of 2.0 ± 2.0 mm, 6.0 ± 2.5 mm, and 1.5 ± 1.5 mm were measured for groups 1 to 3, respectively. No bacterial growth inhibition was observed for group 4 at any time point and none of the other three groups showed inhibition beyond 10 weeks.

FIGURE 4. A) Schematic representation of a Kirby-Bauer antimicrobial test. B) A zone of bacterial growth inhibition indicated eluted antibiotic bioactivity against *S. aureus* growth to 7 weeks for all three groups and up to 9 weeks for Group 2. [Color figure can be viewed in the online issue, which is available at wileyonlinelibrary.com.]

FIGURE 5. Inhibitory Kirby-Bauer ZOI diameters for group 1 to 3 devices are plotted versus time for the Modified Kirby-Bauer analysis. Larger ZOIs correspond to greater antibiotic concentrations. Devices were completely embedded in trypticase soy agar. [Color figure can be viewed in the online issue, which is available at wileyonlinelibrary.com.]
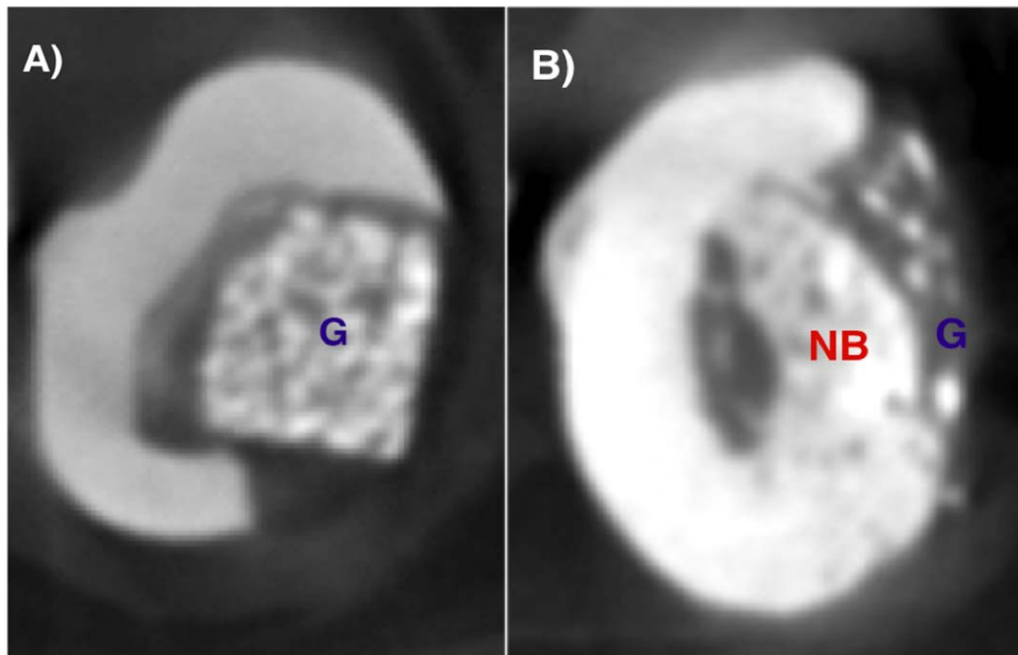
Modified Kirby-Bauer antibiotic susceptibility. All groups except group 4 produced measureable ZOIs for 7 weeks *in vitro* (Figure 5). Average ZOI diameters for the 24-h time point were: 38.7 ± 0.4 mm, 52.8 ± 4.7 mm, and 44.7 ± 1.5 mm for groups 1 to 3, respectively. Statistical difference was confirmed between all three formulations ($p < 0.05$). At 7 weeks, ZOI diameters of 2.0 ± 1.4 mm, 6.7 ± 2.4 mm, and 7.3 ± 0.5 mm were recorded for groups 1 to 3, respectively. Group 2 produced the longest duration of bacterial growth inhibition, exemplified by the production of measureable ZOIs out to 10 weeks. At 10 weeks, ZOI diameters of 2.7 ± 0.9 mm, 12.5 ± 2.6 mm, and 0 ± 0 mm were measured for groups 1 to 3, respectively. At no time point did the group 4 control produce a ZOI.

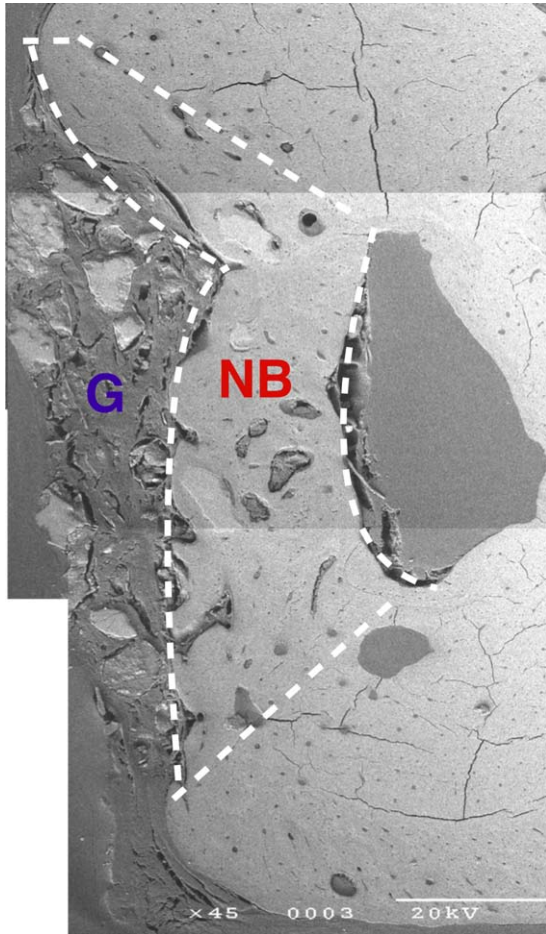**Pilot *in vivo* osteoconductivity assessment**
Micro-CT analysis. As compared with the Time "0" image [Figure 6(A)], 12-week micro-CT analysis of group 3 devices revealed newly formed bone bridging the cortical defect—providing restoration of the medullary canal [Figure 6(B)]. In addition, substantial group 3 device degradation was observed. Also observed was the incorporation of the morselized ProOsteon coralline granule remnants from the group 3 device into the newly formed bone.

BSE image analysis. Following PMMA embedding, the implant-containing region of each radius was divided into four 2-mm thick sections. BSE analysis further substantiated the micro-CT findings for osteoconduction, implant resorption, and integration. New bone was observed to bridge the cortical defect (Figure 7) in three of the four sections prepared for rabbit #102 and all four of the sections for rabbit #103. In the one section that did not exhibit complete bone bridging (#102), a tubular structure, likely a blood vessel, was observed to be running from the endosteal space toward the periosteal surface (figure not shown). ProOsteon was found embedded within the newly formed bone of all sections. The thickness of the ABVF was found to be greatly reduced; with only approximately 0.5 mm of the original 2 mm implant thickness remaining.

MAR analysis. Analysis of bone mineral apposition revealed actively remodeling bone in all samples (Table II), evidenced by the presence of the green fluorescing Calcein in bone (bright regions, Figure 8). Importantly, all sections exhibited accelerated MAR (1.90 ± 0.45–3.36 ± 0.23 μm/day), as

FIGURE 6. *In vivo* Micro-CT image of A) group 3 implants (G) harvested from the radius of a rabbit at time "0." Note the medullary canal was destroyed during the surgical procedure to insert the ABVF device. B) Group 3 ABVF device in the radius of a rabbit after 12 weeks. The destroyed medullary canal was reestablished with new bone (NB) and ProOsteon from the group 3 device was incorporated into the newly formed bone. [Color figure can be viewed in the online issue, which is available at wileyonlinelibrary.com.]

FIGURE 7. Composite image of 12-week Backscatter Electron Microscopy analysis showing repaired cortical bone defect: G = remnant of group 3 device; NB = new bone. White dotted line outlines newly formed. ProOsteon granules are seen scattered throughout the new bone. Thickness of "G" is significantly reduced from original 2-mm ABVF implant thickness. [Color figure can be viewed in the online issue, which is available at wileyonlinelibrary.com.]

compared with the normal MAR of ~1.3 μm/day for New Zealand white rabbits.[31]
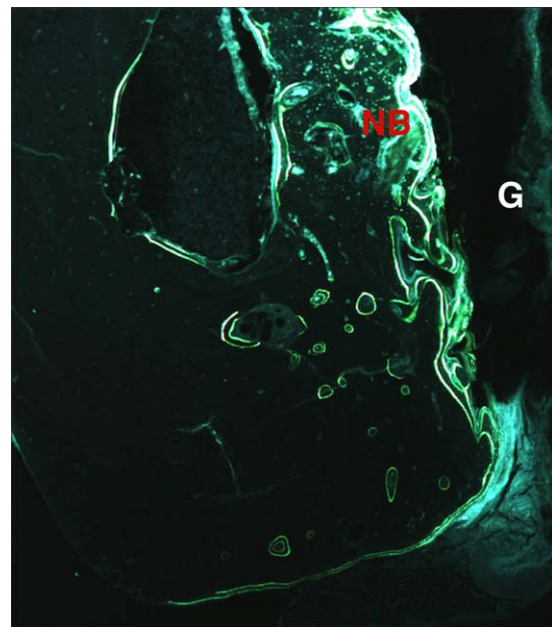
Sanderson's rapid bone stain analysis. Light microscopy also corroborated the findings of the previous (micro-CT, BSE, MAR) analyses indicating bone bridging and integration of the morselized ProOsteon granules in the newly formed bone [Figure 9(A)]. Notably, fibrous tissue was discontinuous and no fibrous capsule was observed. Additional general observations were suggestive of active bone remodeling, characterized by osteoclastic resorption [Figure 9(B) white circle] coupled with new bone formation (NB), characterized by osteoid (white arrow) and osteoblasts on the surface of the osteoid layer [Figure 9(B)]. Although a mild inflammatory response was observed at the periosteal surface, the endosteal surface was characterized by either (1) no inflammatory response—due to absence of the group 3 device, or (2) a local inflammatory response focused on the remaining, unresorbed, group 3 device fragments [Figure

9(C)]. Bone-site macrophages were largely concentrated around the ProOsteon inorganic granules of the group 3 device remnants [Figure 9(D)].
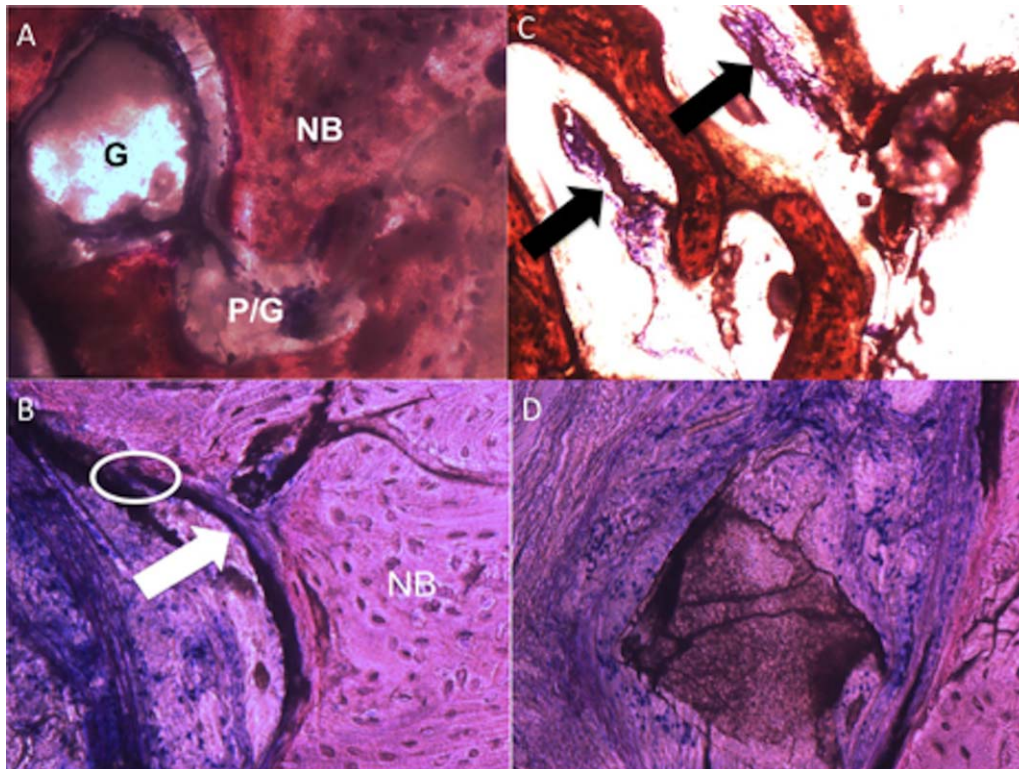
DISCUSSION

Treatment of PJI following total knee arthroplasty continues to challenge clinicians despite advancements in surgical and antimicrobial techniques. Local delivery of antibiotics from degradable combination devices represents potentially promising advantages over current methods utilized to treat these infections.[9,15,17,18,20,24,30,32] A previous *in vivo* study evaluating the group 1 device[20] reported that this device did not degrade *in situ*. Furthermore, the glassy surface of the device provoked a foreign body response resulting in the fibrous encapsulation of the device. This work evaluated three formulations of a resorbable ABVF designed to address the unmet clinical need for a resorbable, osteoconductive, local antibiotic delivery system. Low molecular weight polymer selection was deliberate, as the resorbable implant design is primarily inorganic calcium-based solids where the polymer is used as a binder and degradable encapsulant of the antibiotic drug load for controlled delivery, not as a mechanically robust monolith itself. The device was designed to reduce the risk for recurrent PJI and to restore bone that is lost during surgical debridement in revision total joint replacement procedures.

Following *in vitro* analysis, one of the three formulations was taken forward to examine the device's osteoconductivity *in vivo*. The experimental data produced from this work supported all three hypotheses. Briefly, the three ABVF devices exhibited the ability to elute antibiotic above the

FIGURE 8. Actively mineralizing bone surfaces from group 3 cross-section indicated by osteoblast uptake of calcein green at 16 and 5 days before necropsy using fluorescent microscopy. G = group 3 ABVF device; NB = new bone. [Color figure can be viewed in the online issue, which is available at wileyonlinelibrary.com.]

FIGURE 9. Resorbed antibiotic eluting BVF found incorporated within the new rabbit tibial cortical bone. P = ProOsteon granules from bone void filler, NB = new bone; G = group 3 ABVF device shown to be incorporated into new bone. B) The general appearance of the host bone characterized by osteoclastic resorption (white circle), osteoid (white arrow), and osteoblasts (residing on top of the osteoid layer). C) Arrows illustrate inflammatory response accelerating the rate of device degradation in the endosteal space and the apparent osteoclast resorption of ProOsteon granules. D) Local inflammatory response largely localized around the ProOsteon inorganic coralline granules. All images shown at 20× magnification. [Color figure can be viewed in the online issue, which is available at wileyonlinelibrary.com.]

experimentally determined MIC of *S. aureus* for a minimum of 7 weeks. *In vitro* testing identified group 3 devices as the most rapidly degrading of the three groups, and a pilot *in vivo* analysis of the group 3 devices in rabbit tibia cortical bone revealed extensive bone bridging of the cortical defect, restoration of the medullary canal, and accelerated bone mineral apposition.

Degradable polymers, as a component of the combination device, provided a drug release platform that degraded while eluting antibiotic and gradually produced voids to allow for osteogenesis. To further facilitate new bone formation, a synthetic bone void filler was included to provide an osteoconductive matrix. SEM images showed extensive polymer degradation in the group 3 devices *in vitro* (Figure 3). In contrast, group 1 and 2 devices showed little degradation after 90 days in PBS. The degradation observed in group 3 was an important finding, due to the fact that the group 1 device, previously evaluated *in vivo*,[20] failed to degrade and had elicited a foreign body response—resulting in this device being encapsulated in fibrous tissue. Equally important was the fact that polymer binder degradation resulted in the exposure of the osteoconductive bone void filler ceramic material. These results were not entirely surprising, as salt porogens (for example, calcium chloride used here) are known to yield a less dense polymer matrix and facilitate aqueous media infiltration into the bulk matrix to accel-

erate degradation and dissolution.[33] Furthermore, addition of more rapidly degrading amorphous PLGA compared with more hydrophobic, crystalline PCL,[34] also accelerated the observed degradation of group 3 devices (Figure 3).

In vitro bacterial challenges demonstrated the proliferative ability of the *S. aureus* strain to rapidly reproduce (4-log increase in 24 h) in the experimental environment. The resorbable, ABVFs (groups 1–3) demonstrated the ability to elute antibiotic at concentrations sufficient to eliminate bacterial challenges in excess of 7 weeks *in vitro* using Kirby-Bauer and a Modified Kirby-Bauer antibiotic susceptibility tests (Figures 4 and 5). These *in vitro* results were corroborated by LC-MS/MS analysis, verifying that antibiotic concentrations in the release media remained above the experimentally determined MBC of 3 μg/mL for 7 weeks for groups 1 and 3 and 8 weeks for group 2 [Figure 1(A)].

The antibiotic release profile revealed a maximum tobramycin elution of 97.8 μg/mL (group 1) during the first 24 h [Figure 1(A)]. After 48 h the antibiotic concentration fell to ~20 μg/mL and gradually declined to where it plateaued, above the experimentally determined MBC, at >3.7 μg/mL for the 7 (groups 1 & 3) to 8 (group 2) weeks. Discrete bursts, as observed during the first 24 h, are believed to be beneficial for prophylactic therapy[35] and are able to facilitate eradication of bacteria left behind after debridement in revision procedures.[32] Furthermore, it has been shown that

tobramycin concentrations below 5 mg/mL do not have a significant impact osteoblast viability or proliferative rate.[36]

Group 3 ABVF devices displayed remarkable osteoconductivity and new bone formation (Figure 8), as well as favorable degradation (Figure 9) after 12 weeks *in vivo*. Micro-CT, BSE, and light microscopy all showed bridging of the cortical defect with newly formed bone. ProOsteon® 500R was incorporated into the newly formed bone in a fashion similar to that observed previously[37,38] where ProOsteon 200R was coupled with Osteogenic Protein-1 to achieve significant bone apposition, comparable to allograft, within a surgically created defect in a Labrador femoral condyle model. These study findings were also supported by the results of others[12] who used PDLA-CaCO$_3$ sleeves to repair 2.5 to 3.0 cm mid-diaphyseal defects in the middle third of the Yucatan minipig radius, where the sleeve served as a structural scaffold for bone regeneration and ultimately enhanced bone healing.

Although these outcomes show promise, this study was not without limitations. To achieve statistically relevant data, numbers of rabbits will need to be increased from this pilot two to seven (97% confidence) per group. Additionally, the bactericidal efficacy of the ABVF device will also need to be tested *in vivo* to ensure that the device possesses both osteoconductive and antimicrobial properties in the infected rabbit implant model and more relevant implant revision model. Finally, evaluation of the device in cancellous bone and an animal model that more closely resembles the human weight and bone remodeling rate will provide more accurate indications of the device's ability to reduce rates of PJI while restoring bone lost to debridement in current revision total joint replacement procedures.

CONCLUSIONS

These studies demonstrate the *in vitro* bactericidal activity and resorbability of the three groups of antibiotic-eluting bone void filler devices, as well as their *in vivo* osteoconductivity in a rabbit implant model. *In vitro* studies demonstrate the ability of these devices to eliminate *S. aureus* bacterial challenges up to 5×10^8 CFU/mL and showed significant degradation (group 3 devices) after 10 weeks in PBS solution. Group 3 devices demonstrated the most desirable resorptive properties and drug elution kinetics of the three groups and were taken forward for *in vivo* testing in the rabbit radius. The *in vivo* osteoconductivity challenge utilizing group 3 devices demonstrated extensive new bone formation after 12 weeks. Evaluation of the periprosthetic host tissue revealed an increased bone mineral apposition rate when compared with the average of 1.3 μm/day. This finding was both advantageous and indicative of the fact that bone formation was not adversely affected by local, extended release of tobramycin. In future studies, group sizes will be increased to ensure the generation of statistically significant data. Additionally, the ABVF device will be challenged in a sheep femoral condyle implant model to better approximate the weight and bone remodeling rate of humans.

REFERENCES

1. Garvin KL, Konigsberg BS. Infection following total knee arthroplasty: Prevention and management. J Bone Joint Surg Am 2011; 93:1167–1175.
2. Kurtz SM, Lau E, Watson H, Schmier JK, Parvizi J. Economic burden of periprosthetic joint infection in the United States. J Arthroplasty 2012;27:e61–e65.
3. Trampuz A, Widmer AF. Infections associated with orthopedic implants. Curr Opin Infect Dis 2006;19:349–356.
4. Fletcher MD, Spencer RF, Langkamer VG, Lovering AM. Gentamicin concentrations in diagnostic aspirates from 25 patients with hip and knee arthroplasties. Acta Orthop Scand 2004;75:173–176.
5. Powles JW, Spencer RF, Lovering AM. Gentamicin release from old cement during revision hip arthroplasties. J Bone Joint Surg Br 1998;80:607–610.
6. Lew DP, Waldvogel FA. Osteomyelitis. Lancet 2004;364:369–379.
7. Sierink J, Schep N, Terra M, Luitse J, Goslings J. A case of sequester and involucrum formation of the fibula. J Med Cases 2012;3:7–11.
8. Costerton JW, Stewart PS, Greenberg EP. Bacterial biofilms: A common cause of persistent infections. Science 1999;284:1318–1322.
9. Meani E, Romano C. Treatment of osteomyelitis by local antibiotics using a portable electronic micropump. Rev Chir Orthop Reparatrice Appar Mot 1994;80:285–290.
10. Soundry M, Greental A, Nierenberg G, Falah M, Rosenberg N. Periprosthetic Infection Following Total Knee Arthroplasty. InTech. 2013. Available at: http://www.intechopen.com/books/arthroplasty-update/periprosthetic-infection-following-total-knee-arthroplasty.
11. Gunatillake PA, Adhikari R. Biodegradable synthetic polymers for tissue engineering. Eur Cells Mater 2003;5, 1–16; discussion 16.
12. Meinig RP, Buesing CM, Helm J, Gogolewski S. Regeneration of diaphyseal bone defects using resorbable poly(L/DL-lactide) and poly(D-lactide) membranes in the Yucatan pig model. J Orthop Trauma 1997;11:551–558.
13. Laurencin CT, Gerhart T, Witschger P, Satcher R, Domb A, Rosenberg AE, Hanff P, Edsberg L, Hayes W, Langer R. Bioerodible polyanhydrides for antibiotic drug delivery: In vivo osteomyelitis treatment in a rat model system. J Orthop Res 1993;11:256–262.
14. Hafeman AE, Zienkiewicz KJ, Carney E, Litzner B, Stratton C, Wenke JC, Guelcher SA. Local delivery of tobramycin from injectable biodegradable polyurethane scaffolds. J Biomater Sci Polym Ed 2010;21:95–112.
15. Hendricks KJ, Lane D, Burd TA, Lowry KJ, Day D, Phaup JG, Anglen JO. Elution characteristics of tobramycin from polycaprolactone in a rabbit model. Clin Orthop Relat Res 2001;392:418–426.
16. Mourino V, Boccaccini AR. Bone tissue engineering therapeutics: Controlled drug delivery in three-dimensional scaffolds. J R Soc Interface 2010;7:209–227.
17. Schlickewei CW, Yarar S, Rueger JM. Eluting antibiotic bone graft substitutes for the treatment of osteomyelitis in long bones. A review: Evidence for their use? Orthop Res Rev 2014;2014:71–79.
18. Brooks BD, Sinclair KD, Davidoff SN, Lawson S, Williams AG, Coats B, Grainger DW, Brooks AE. Molded polymer-coated

composite bone void filler improves tobramycin controlled release kinetics. J Biomed Mater Res B 2013;102:1074–1083.

19. Keevil B, Lockhart SJ, Cooper D. Determination of tobramycin in serum using liquid chromatography-tandem mass spectrometry and comparison with fluorescence polarization assay. J Chromatogr B Anal Technol Biomed Life Sci 2003;794:329–335.

20. Brooks BD, Sinclair KD, Grainger DW, Brooks AE. A resorbable antibiotic-eluting polymer composite bone void filler for perioperative infection prevention in a rabbit radial defect model. PLOS One 2015;10:e0118696.

21. Ellington JK, Harris M, Webb L, Smith B, Smith T, Tan K, Hudson M. Intracellular *Staphylococcus aureus*. A mechanism for the indolence of osteomyelitis. J Bone Joint Surg Br 2003;85:918–921.

22. Cockerill FR, William M, Alder J, Dudley MN, Eliopoulos GM, Ferraro MJ, Hardy DJ, Hecht DW, Hindler JA, Patel JB, Powell M, Swenson JM, ThomsonJr. RB, Traczewski MM, Turnidge JD, Weinstein MP, Zimmer BL. Methods for Dilution Antimicrobial Susceptibility Tests for Bacteria That Grown Aerobically; Approved Standard, 9th ed., CLSI document M07-A9. Wayne, PA: Clinical and Laboratory Standards Institute; Vol.32. 2006.

23. Bauer AW, Perry DM, Kirby WM. Single-disk antibiotic-sensitivity testing of staphylococci; an analysis of technique and results. Arch Int Med 1959;104:208–216.

24. Sinclair KD, Pham TX, Williams DL, Farnsworth RW, Loc-Carrillo CM, Bloebaum RD. Model development for determining the efficacy of a combination coating for the prevention of perioperative device related infections: a pilot study. J Biomed Mater Res B 2013;101:1143–1153.

25. Bloebaum RD, Bachus KN, Momberger NG, Hofmann AA. Mineral apposition rates of human cancellous bone at the interface of porous coated implants. J Biomed Mater Res 1994;28:537–544.

26. Bloebaum RD, Willie B, Mitchell BS, Hofmann AA. Relationship between bone ingrowth, mineral apposition rate, and osteoblast activity. J Biomed Mater Res A 2007;81:505–514.

27. Wang X, Michoel A, Van den Mooter G. Study of the phase behavior of polyethylene glycol 6000-itraconazole solid dispersions using DSC. Int J Pharm 2003;272:181–187.

28. Fonseca CP, Cavalcante JF, Amaral FA, Souza CAZ, Neves S. Thermal and conduction properties of a PCL-biodegradable gel polymer electrolyte with LiClO4, LiF3CSO3, and LiBF4 Salts. Int J Electrochem Sci 2007;2:52–63.

29. Bala I, Hariharan S, Kumar MNVR. PLGA nanoparticles in drug delivery: The state of the art. Crit Rev Therap Drug Carrier Syst 2004;21:387–422.

30. Ambrose CG, Clyburn TA, Louden K, Joseph J, Wright J, Gulati P, Gogola GR, Mikos AG. Effective treatment of osteomyelitis with biodegradable microspheres in a rabbit model. Clin Orthop Relat Res 2004;421:293–299.

31. Hirano T, Burr DB, Turner CH, Sato M, Cain RL, Hock JM. Anabolic effects of human biosynthetic parathyroid hormone fragment (1-34), LY333334, on remodeling and mechanical properties of cortical bone in rabbits. J Bone Miner Res 1999;14:536–545.

32. Kundu B, Nandi SK, Roy S, Dandapat N, Soundrapandian C, Datta S, Mukherjee P, Mandal TK, Dasgupta S, Basu D. Systematic approach to treat chronic osteomyelitis through ceftriaxone-sulbactam impregnated porous-tricalcium phosphate localized delivery system. Ceram Int 2012;38:1533–1548.

33. Barbanti S, Zavaglia C, de Rezende Duek E. Effect of salt leaching on PCL and PLGA (50/50) resorbable scaffolds. Mater Res 2008;11: 75–80.

34. Sabir M, Xu X, Li L. A review on biodegradable polymeric materials for bone tissue engineering applications. J Mater Sci 2009;44: 5713–5724.

35. Stallmann HP, Faber C, Bronckers ALJJ, Amerongen AVN, Wuisman PIJM. In vitro gentamicin release from commercially available calcium-phosphate bone substitutes in fluence of carreier type on duration of the releasae profile. BMC Musculoskelet Disord 2006;7:1–8.

36. Rathbone CR, Cross JD, Brown KV, Murray CK, Wenke JC. Effect of various concentrations of antibiotics on osteogenic cell viability and activity. J Orthop Res 2011;29:1070–1074.

37. Jensen TB, Overgaard S, Lind M, Rahbek O, Bunger C, Soballe K. Osteogenic protein-1 increases the fixation of implants grafted with morcellised bone allograft and ProOsteon substitute: An experimental study in dogs. J Bone Joint Surg Br 2007;89:121–126.

38. Jensen TB, Overgaard S, Lind M, Rahbek O, Bunger C, Soballe K. Osteogenic protein 1 device increases bone formation and bone graft resorption around cementless implants. Acta Orthop Scand 2002;73:31–39.